

# Nonadiabatic Molecular Dynamics Simulations of Correlated Electrons in Solution. 1. Full Configuration Interaction (CI) Excited-State Relaxation Dynamics of Hydrated Dielectrons

Ross E. Larsen and Benjamin J. Schwartz\*

Department of Chemistry and Biochemistry, University of California, Los Angeles, California 90095-1569

Received: September 19, 2005; In Final Form: October 25, 2005

The hydrated dielectron is composed of two excess electrons dissolved in liquid water that occupy a single cavity; in both its singlet and triplet spin states there is a significant exchange interaction so the two electrons cannot be considered to be independent. In this paper and the following paper, we present the results of mixed quantum/classical molecular dynamics simulations of the nonadiabatic relaxation dynamics of photoexcited hydrated dielectrons, where we use full configuration interaction (CI) to solve for the two-electron wave function at every simulation time step. To the best of our knowledge, this represents the first systematic treatment of excited-state solvation dynamics where the multiple-electron problem is solved exactly. The simulations show that the effects of exchange and correlation contribute significantly to the relaxation dynamics. For example, spin-singlet dielectrons relax to the ground state on a time scale similar to that of single electrons excited at the same energy, but spin-triplet dielectrons relax much faster. The difference in relaxation dynamics is caused by exchange and correlation: The Pauli exclusion principle imposes very different electronic structure when the electrons' spins are singlet paired than when they are triplet paired, altering the available nonadiabatic relaxation pathways. In addition, we monitor how electronic correlation changes dynamically during nonadiabatic relaxation and show that solvent dynamics cause electron correlation to evolve quite differently for singlet and triplet dielectrons. Despite such differences, our calculations show that both spin states are stable to excited-state dissociation, but that the excited-state stability has different origins for the two spin states. For singlet dielectrons, the stability depends on whether the solvent structure can rearrange to create a second cavity before the ground state is reached. For triplet dielectrons, in contrast, electronic correlation ensures that the two electrons do not dissociate, even if the dielectron is artificially kept from reaching the ground state. In addition, both singlet and triplet dielectrons change shape dramatically during relaxation, so that linear response fails to describe the solvation dynamics for either spin state. In the following paper (Larsen, R. E.; Schwartz, B. J. *J. Phys. Chem. B* 2006, 110, 9692), we use these simulations to calculate the pump–probe spectroscopic signal expected for photoexcited hydrated dielectrons and to predict an experiment to observe hydrated dielectrons directly.

## I. Introduction

Despite the fact that most molecules possess multiple electrons, the vast majority of computer simulations of excited-state relaxation in the condensed phase make the approximation that there is only a single important electronic degree of freedom and that the nuclei may be treated classically.<sup>1–7</sup> Since only a single electronic degree of freedom is treated explicitly, the effects of the remaining electrons must be included in some approximate fashion, usually by the use of a pseudopotential.<sup>8</sup> This type of single-electron picture ought to be limited to systems in which the electron being treated explicitly and those being treated implicitly are not correlated, but unfortunately, this does not describe the electronic structure of most molecules or even of atoms that have more than a single valence electron. For example, despite a large effort in single-electron simulations of the charge-transfer-to-solvent (CTTS) of photoexcited iodide in water,<sup>9</sup> Bradforth and Jungwirth recently have shown that the electronic structure of hydrated iodide is not properly described by a single-electron picture:<sup>10</sup> correlation among the valence electrons of iodide precludes an accurate single-electron treatment of CTTS. Likewise, an accurate description of

molecular bonding also depends on the inclusion of electron–electron interactions; even the potential energy surfaces of a molecule as simple as H<sub>2</sub> cannot be correctly described without an explicit inclusion of electron correlation.<sup>11</sup> Many-electron effects have been included in a few condensed-phase simulations semiempirically,<sup>12</sup> with Hartree–Fock,<sup>13</sup> and with time-dependent density functional theory;<sup>14,15</sup> it is not clear, however, how accurate the excited states are for a given electronic structure approximation or exchange–correlation functional, therefore it is not obvious that these approaches will be able to produce correct excited-state dynamics and relaxation for all systems.

Ideally, one would circumvent such difficulties simply by calculating condensed-phase nonadiabatic relaxation dynamics using the full many-electron electronic structure for every time step of a molecular dynamics simulation. Then electron correlation would be included exactly and there would be no need to subsume correlation into some single-electron effective repulsive potential or some approximate exchange–correlation functional. In this paper we achieve this ideal, albeit for a condensed-phase system with only two electrons, by solving the electronic structure problem *exactly* with full configuration interaction (CI). The full CI solutions allow us to examine the role of electron correlation in solution-phase relaxation dynamics

\* Corresponding author.

with unprecedented detail and accuracy. Furthermore, we will calculate the excited-state dynamics of both singlet-paired electrons and triplet-paired electrons, thus investigating how the Pauli exclusion principle and spin statistics influence nonadiabatic relaxation and solvation.

The species whose dynamics we examine in this paper is the simplest possible two-electron condensed-phase solute: the hydrated dielectron.<sup>16–19</sup> Like its one-electron analogue, the hydrated electron,<sup>20–25</sup> the hydrated dielectron serves as an excellent probe of solvation dynamics because its electronic properties are determined entirely by the solvent, but the dielectron has the added advantage of including all of the exchange and correlation effects that are characteristic of multielectron systems. Recently, we have reported detailed simulation results of the equilibrium structure and dynamics of this two-electron solvent-supported species.<sup>19</sup> We found that the hydrated dielectron possesses two distinct configurations, which correspond to the two electrons being either singlet or triplet paired. For the singlet dielectron, both electrons occupy a single, potato-shaped cavity in the water and have  $\sim 2$  eV of correlation energy, whereas for the triplet case, the two electrons share a peanut-shaped cavity and have about half the exchange energy of the singlet case. In this paper, we simulate the properties of hydrated dielectrons following electronic excitation in order to examine rigorously how exchange and correlation affect condensed-phase nonadiabatic relaxation and solvation dynamics. In the following paper,<sup>46</sup> henceforth referred to as Paper II, we will use these simulations to calculate the transient spectroscopy of hydrated dielectrons and to suggest a pump–probe experiment to observe dielectrons directly.

The rest of this paper is organized as follows. Section II describes details of the model and computational methods used to solve the two-electron problem using full CI. In section III we describe the relaxation dynamics of both singlet and triplet hydrated dielectrons following excitation from the ground to a higher-lying (di)electronic state. We find that both singlet and triplet dielectrons undergo significant size and shape changes as they relax and that these changes are accompanied by large changes in electronic structure (e.g., in the amount of diradical character of the occupied excited state). We also show that although neither singlet nor triplet dielectrons dissociate after excitation due to rapid nonadiabatic relaxation to the ground state, the relaxation dynamics of the singlet dielectron is very different from that of the triplet dielectron; this difference results entirely from the constraints imposed by the Pauli exclusion principle for each spin state. In addition, we find that linear response does not describe the solvation dynamics of dielectrons, a result that is perhaps not unexpected in view of the significant size and shape changes during relaxation. Section IV presents a discussion of all of the results.

## II. Model and Computational Details

The simulation techniques used for the full CI nonadiabatic dynamics reported in this paper have been described in detail elsewhere,<sup>18,19</sup> so here we give only a brief summary of our model and computational methods. We have run constant-energy mixed quantum/classical (QM/CM) molecular dynamics simulations at a temperature of  $\sim 300$  K in a cubic box  $18.17 \text{ \AA}$  on a side that contains 200 classical water molecules and two excess electrons; all interactions were computed using minimum-image periodic boundary conditions<sup>26</sup> with the interactions tapered smoothly to zero at half the box length.<sup>27,28</sup> The classical water dynamics and intermolecular interactions were propagated using the velocity Verlet algorithm with a time step of 0.5 fs, and the

inter- and intramolecular interactions of the water were given by the SPC/Flex potential.<sup>29</sup> The forces that the quantum mechanical electrons exert on the classical particles are of the Hellmann–Feynman form, so that the size and shape of the two-electron charge density determines the force on each water molecule due to interaction with the dielectron.<sup>18</sup> The two excess electrons repel each other through the Coulomb interaction, and they interact with the solvent molecules through a pairwise pseudopotential introduced by Schnitker and Rossky;<sup>20</sup> although more accurate electron-water pseudopotentials are known,<sup>22</sup> this choice allows for direct comparison to the extensive simulation literature of the hydrated electron performed using this pseudopotential.<sup>21,23</sup>

For each water configuration, we compute the adiabatic two-electron eigenstates of the system using full configuration interaction (CI), as described in detail in refs 18 and 19. Briefly, at every simulation time step, each adiabatic two-electron eigenstate is expanded in a series of antisymmetrized products of single-electron adiabatic eigenstates,

$$|\Psi_i\rangle = \sum_{n,m} c_{n,m}^{i,\pm} |n, m\rangle_{\pm} \quad (1)$$

where  $|n, m\rangle_{\pm} = (|n\rangle_1|m\rangle_2 \pm |m\rangle_1|n\rangle_2)/\sqrt{2}$ ,  $|n, n\rangle_+ = |n\rangle_1|n\rangle_2$ , and  $|n\rangle_k$  denotes a single electron eigenstate for electron  $k$ ; the plus sign denotes spin singlet dielectrons and the minus sign spin triplet dielectrons, with  $m \geq n$  for the singlet and  $m > n$  for the triplet case. For every solvent configuration we calculate the  $N = 10$  lowest single-electron adiabatic eigenstates on a  $16 \times 16 \times 16$  cubic grid with an iterative-and-block-Lanczos procedure.<sup>30</sup> We then compute the two-electron adiabatic eigenstates with full CI using a basis of  $N(N \pm 1)/2$  appropriately symmetrized two-electron product basis states.<sup>31</sup> The electron–electron Coulomb and exchange interactions needed for full CI were computed using the efficient real-space quadrature that we introduced in ref 18. We achieved an additional increase in speed by making what we have called the “important states” approximation,<sup>18</sup> in which we perform the full CI calculation only every 3 fs (6 time steps), constructing a smaller CI matrix at intermediate times using a subset of the two-electron product basis states that we refer to as the important states. Here, the important states comprise all two-electron product states needed to represent 99.95% of the occupied two-electron eigenstate and 99% of the rest of the 10 lowest-energy unoccupied two-electron eigenstates. We have not allowed intersystem crossings in the simulations reported here, so the two electrons were constrained to be either fully singlet or triplet at all times. Note that our choice of the grid basis rather than a more standard molecule-based basis prevents any bias in terms of whether the dielectrons prefer to be together or apart, or on top of or between the solvent molecules; the grid basis set is flexible enough to allow the dielectrons to change size and shape or even dissociate.

The nonadiabatic dynamics of the two-electron system were calculated using Prezhdo and Rossky’s mean-field with surface-hopping (MF/SH) algorithm.<sup>5</sup> In this algorithm, which combines Tully’s fewest switches method<sup>2</sup> with Ehrenfest dynamics, the initially occupied adiabatic state is taken to be the “reference state” and the wave function of the system evolves coherently according to the time-dependent Schrödinger equation (mean-field dynamics). When certain criteria are met, the wave function is collapsed either to the reference state (mean-field rescaling) or stochastically to a new state (a surface hop), which then becomes the reference state. Details of our implementation of the MF/SH algorithm for two-electron systems may be found in ref 18.<sup>32</sup>

For both singlet and triplet dielectrons, we have run 30 nonequilibrium trajectories using uncorrelated initial configurations taken from 30-ps-long singlet and triplet adiabatic trajectories.<sup>19</sup> For each nonequilibrium trajectory, the dielectron was promoted from the ground state to a resonant excited state that was  $4.00 \pm 0.01$  eV above the ground state. We chose the 4.0-eV excitation energy because our simulations have shown<sup>19</sup> that both the singlet and triplet dielectrons have significant oscillator strength at this wavelength but the (single) hydrated electron does not. Thus, our simulations are designed to mimic a pump–probe experiment where the pump energy is chosen to be largely to the blue of the hydrated electron’s absorption band (see ref 19); as we discuss below and in Paper II,<sup>49</sup> we believe that these are the ideal experimental conditions under which to spectroscopically verify the existence of hydrated dielectrons.

### III. Exchange and Correlation in the Excited-State Relaxation Dynamics of Hydrated Dielectrons

In this section, we investigate the relaxation dynamics of both singlet and triplet hydrated dielectrons after 4.0-eV excitation from the ground electronic state. We examine both individual trajectories and nonequilibrium ensemble average properties in detail, and explore how the presence of exchange and correlation in this system affects linear response. As noted above, our simulations do not include the possibility of intersystem crossing, so we shall discuss the dynamics of each of the two spin states separately.

**A. Relaxation Dynamics of the Photoexcited Singlet Hydrated Dielectron.** We found in our previous study of the equilibrium dynamics of hydrated dielectrons that the singlet dielectron is energetically more stable than the triplet dielectron, although the triplet dielectron does appear to be kinetically stable on the time scale of our simulations.<sup>19</sup> Moreover, we recently have completed a detailed study of the thermodynamics of hydrated electrons and dielectrons,<sup>33</sup> and as a result, we believe that singlet dielectrons are much more likely to exist experimentally than triplets. Thus, in this subsection we discuss the behavior of photoexcited singlet hydrated dielectrons in detail.

*1. Results: Full-CI Nonadiabatic Nonequilibrium Mixed Quantum/Classical Trajectories of Singlet Hydrated Dielectrons.* Figure 1a displays a dynamical history of the adiabatic eigenstates (shown as alternating dotted and solid gray curves) and the occupied mean-field state (heavy solid curve) for a typical nonequilibrium trajectory following 4.0-eV excitation of the equilibrated singlet hydrated dielectron. In this trajectory, following promotion of the equilibrium dielectron to the (resonant) seventh excited state at  $t = 0$ , the excited dielectron mixes strongly with the nearby excited states and undergoes a series of nonadiabatic transitions to reach the lowest excited state after  $\sim 70$  fs. After this time, there is little mixing with any of the higher-lying excited states, which have increased in energy relative to the occupied state, but significant mixing with the ground state occurs as the ground state energy rises, so that in this trajectory the system eventually internally converts to the ground state after  $\sim 500$  fs. Figure 2a shows the dynamical history of the occupied- and ground-state energies averaged over all 30 nonequilibrium trajectories while the dielectron occupies one of the excited states.<sup>34</sup> This figure shows that the energy of the occupied state of the excited dielectron decreases in a rapid cascade of nonadiabatic transitions until it reaches the first excited state; during this cascade, the ground-state energy rises as the solvent moves to stabilize the altered excited-state charge density. A fit of each average energy curve to a single

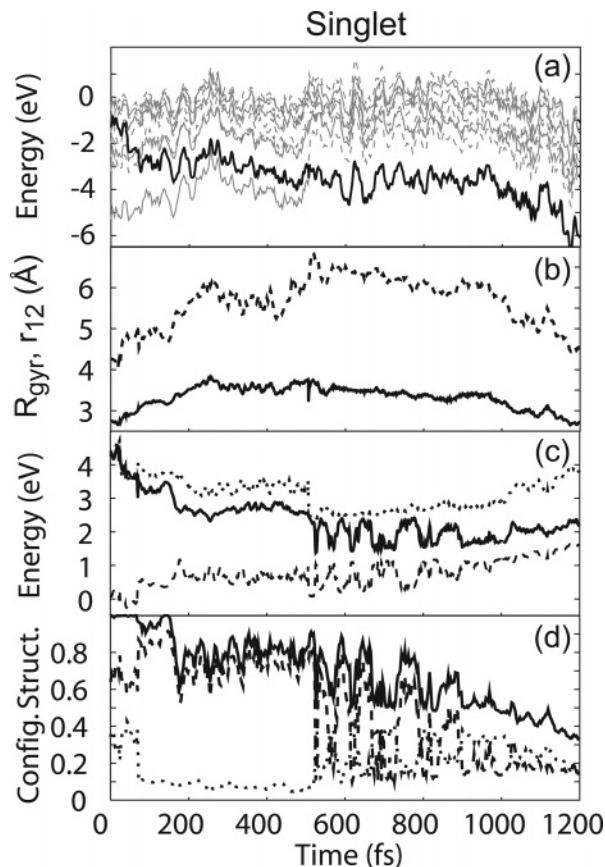


**Figure 1.** Representative dynamical history of nonadiabatic relaxation by a singlet dielectron following resonant 4.0 eV excitation at time  $t = 0$ . Panel a: Adiabatic energy levels (alternating thin gray solid and dashed curves) and mean-field energy (thick black curve). Panel b: Radius of gyration ( $R_{\text{gyr}}$ , solid curve) and electron–electron separation ( $r_{12}$ , dashed curve) of the occupied adiabatic state. Panel c: Coulomb (solid curve) and exchange (dashed curve) energies of the occupied adiabatic eigenstate, and their sum (dotted curve), the total interaction energy. Panel d: Fraction of excited-state (solid curve), radical (dashed curve) and diradical (dotted curve) character of the occupied adiabatic eigenstate, defined as described in Section III.A.2.

exponential (dashed curves) yields a  $\sim 1$  eV average excited-state energy decrease on a time scale of 50 fs, and a  $\sim 2$  eV increase in the average ground-state energy on a time scale of 130 fs.<sup>35</sup>

Figure 1b displays the radius of gyration,  $R_{\text{gyr}}$  (solid curve), and the average interelectron separation,  $r_{12} = \sqrt{\langle \Psi | |\mathbf{r}_1 - \mathbf{r}_2|^2 | \Psi \rangle}$  (dashed curve), of the occupied state for the prototypical excited singlet-dielectron trajectory whose energy-level history is shown in Figure 1a; details of how these quantities are calculated using multielectron wave functions are found in ref 19. Although both quantities fluctuate, neither undergoes a significant change in the first several hundred fs after excitation, indicating that the Franck–Condon excitation leaves the excited dielectron in essentially the same cavity as the ground state. After the system reaches the first excited state at  $\sim 300$  fs, however, the radius of gyration and the interelectron separation both increase steadily until the system makes the transition to the ground state at  $\sim 530$  fs. Following the nonadiabatic transition to the ground state, the system reequilibrates within 700 fs. Figure 2b shows the dynamics of the radius of gyration (solid curve) and the interelectron separation (dashed curve) averaged over all 30 of the nonequilibrium excited-state runs. The radius of gyration and the interelectron separation increase steadily by  $\sim 25\%$  over the first 500 fs and then level

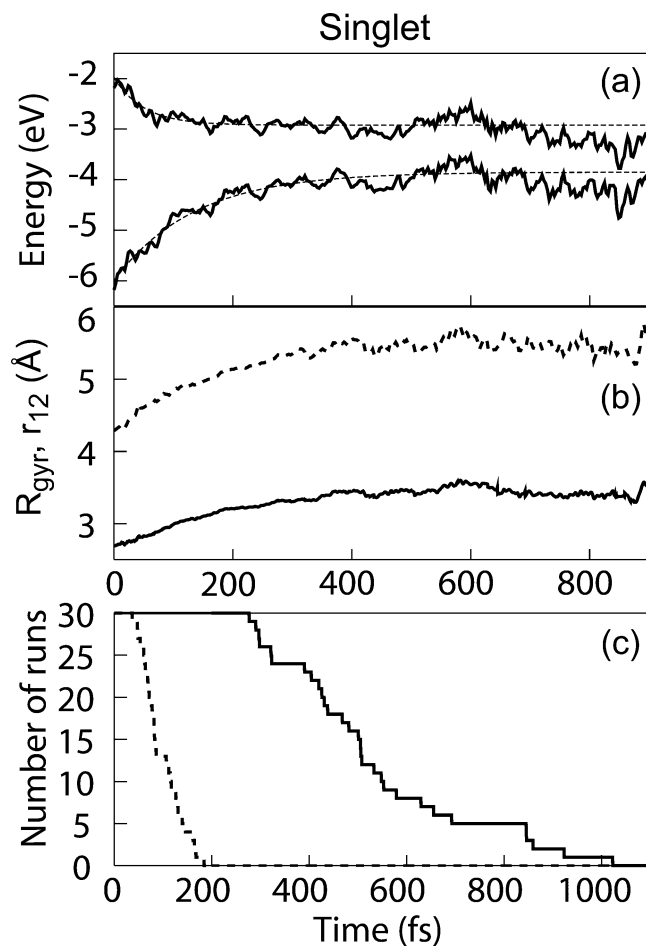


**Figure 2.** Nonequilibrium average dynamics for singlet dielectron relaxation following 4.0 eV excitation at time  $t = 0$ . Panel a: Average energies of the occupied excited state and the ground state after excitation (solid curves).<sup>34</sup> The dashed curves show single-exponential fits, with time constants of 134 and 50 fs, respectively, for the ground and mean-field energies.<sup>35</sup> Panel b: Average radius of gyration ( $R_{\text{gyr}}$ , solid curve) and interelectron separation ( $r_{12}$ , dashed curve) of the occupied excited state. Panel c: Number of singlet-dielectron runs above the ground state (solid curve) and above the first excited state (dotted curve) as a function of time after excitation.

off. Both of these trends suggest that the excited-state electrons are trying to separate, but for the reasons discussed further below, the two electrons are able to get only  $\sim 5.5$  Å apart on average before the system returns to the ground state.

To better visualize the electronic changes that take place during the nonequilibrium dynamics, Figure 3 displays contour plots of the charge densities of both the occupied and ground electronic states at a few select times during the relaxation for the trajectory studied in Figure 1. We chose to display the charge density of the ground state as well as the occupied state because the repulsive form of the electron–water pseudopotential near the water molecules means that the ground-state density only occupies regions where there are no water molecules, providing a convenient way to visualize the “cavity” carved out by the dielectron.<sup>21</sup> At the time of excitation, the occupied excited state (shown in yellow) is somewhat larger and less spherical than the ground state (shown in red), but the excited state clearly occupies the same solvent cavity as the ground state. By 180 fs after excitation, the occupied excited state has developed two lobes and the cavity it occupies (as revealed by the ground state charge density) has lengthened significantly. By 360 fs the smaller of the two lobes has grown and the ground state has shrunk in response to rearrangement of the first solvation shell.

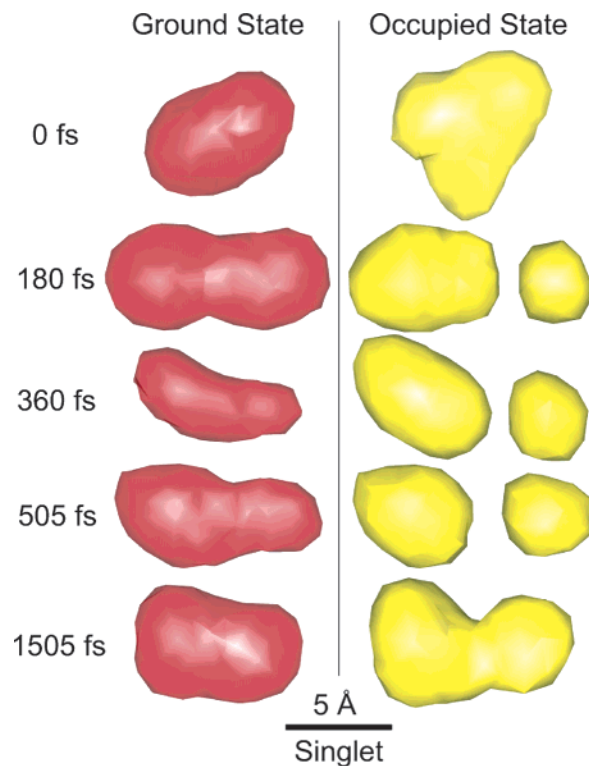


**Figure 3.** Charge density contours of the occupied and ground state for the singlet run shown in Figure 1. The ground-state charge density is displayed in red and the occupied-state charge density in yellow for the times indicated; in both cases the contours are drawn at a charge density of 10 of the maximum charge density for the state displayed. The “occupied state” contour at time  $t = 1505$  fs displays the *unoccupied* first excited state, because the occupied state at this time is the ground state.

Finally, immediately before the nonadiabatic transition to the ground state, the occupied excited state has evolved into two separate lobes of unequal size. The two lobes are *not* separated single hydrated electrons, however, because the ground-state charge density (and our examination of individual configurations using molecular visualization software) shows clearly that no water molecules reside in the space between the two lobes. Moreover, as we will discuss in the next subsection, the two electrons still have a significant exchange energy at this time, indicating that they act as a single, correlated quantum mechanical entity rather than as two individual electrons. Following the nonadiabatic transition to the ground state, the dielectron returns to its equilibrium “potato” shape.<sup>19</sup>

We turn next in our study of the singlet dielectron’s relaxation dynamics to examining the excited-state lifetimes of all 30 of our nonequilibrium trajectories. Figure 2c shows the total number of trajectories in which the MF/SH reference state is either above the ground state (solid curve) or above the first excited state (dotted curve) as a function of time following excitation. On average, the 4.0 eV excited singlet dielectron takes 100 fs to reach the first excited state with an average excited-state lifetime of 530 fs; see Table 1. This average excited-state lifetime is  $\sim 200$  fs shorter than to that seen in simulations following the  $\sim 2.3$  eV excitation of a hydrated electron,<sup>21</sup> and we turn in the next subsection to the question of how the dielectron is able to dissipate nearly twice as much energy on a slightly faster time scale as the single electron.

**2. Discussion: The Roles of Exchange and Correlation in the Relaxation Dynamics of the Singlet Hydrated Dielectron.** We begin our discussion by addressing the question of how the excited singlet hydrated dielectron is able to return so quickly

**TABLE 1: Average Excited-State Lifetimes and Uncertainties for Excited Hydrated Dielectrons<sup>a</sup>**

spin state	time to 2 (fs) <sup>b</sup>	time from 2 to 1 (fs) <sup>c</sup>	time to 1 (fs) <sup>d</sup>
singlet	98 (15)	434 (73)	532 (73)
triplet	123 (25)	45 (17)	161 (23)

<sup>a</sup> The numbers in parentheses are two standard deviation errors. <sup>b</sup> Time after excitation for the first excited state to be reached, calculated from 30 (27) runs for singlet (triplet) dielectrons. <sup>c</sup> Time between the first excited-state being reached and the transition to the ground state, calculated from 30 (27) runs for singlet (triplet) dielectrons. <sup>d</sup> Time after excitation until the transition to the ground state, calculated from 30 runs for both singlet and triplet dielectrons.

to its electronic ground state. Unlike the hydrated electron, which has only three cavity-bound excited states, the dielectron has well over a dozen cavity-bound excited states because the attractive potential of the cavity is much deeper than for the single electron.<sup>19</sup> The 130-fs time scale on which the ground-state energy of the excited singlet dielectron increases following excitation (cf. Figure 2a) is faster than that of the photoexcited hydrated electron,<sup>21</sup> indicating that the solvent must accommodate the excited-state charge distribution in regions previously occupied by solvent molecules. The excited hydrated electron, in contrast, is solvated by water moving into empty regions that were previously occupied by the electronic ground state.<sup>21</sup> It has been well documented that the solvation dynamics of SPC/Flex water are faster when the solute increases in size than when the solute decreases in size, due to the nature of the different solvent motions involved.<sup>36</sup> Thus, there are two reasons the singlet dielectron is able to dissipate the excitation energy more rapidly than the hydrated electron: First, the fact that nonadiabatic transitions are quite facile through the dense manifold of dielectron excited states provides an extra  $\sim 1$  eV of stabilization to close the gap, and second, the size increase of the dielectron's excited state leads to faster destabilization of the ground-state energy.

Now that we see that solvation dynamics destabilizes the ground state of the singlet dielectron while nonadiabatic relaxation simultaneously lowers the energy of the occupied excited state, we turn next to the question of how the electron correlation changes during this relaxation. Figure 1c shows the Coulomb (solid curve) and exchange (dashed curve) energies for our representative excited singlet-dielectron trajectory as well as their sum, the total electron–electron interaction energy (dotted curve).<sup>37</sup> We see that the exchange energy drops to near zero upon excitation, suggesting that the excitation is one-electron in character: by exciting predominantly only one of the electrons, the correlation between them is largely removed. Following the rapid nonadiabatic cascade to the first excited state after  $\sim 70$  fs, however, the exchange energy rises to roughly  $\sim 15\%$  of the Coulomb energy, so that nonadiabatic relaxation increases the correlation between the electrons. Over the next few hundred femtoseconds, the average interelectron separation increases, (cf. Figure 1b) causing the Coulomb interaction between the electrons to decrease. The exchange interaction between the electrons increases at essentially the same rate as the Coulomb energy decreases, however, so that on average the total interaction energy remains roughly constant. With our definition of the exchange energy,<sup>37</sup> the near constancy of the average total electron interaction energy tells us that during relaxation, the two-electron wave function is gaining amplitude from configurations in which both electrons occupy the same single-electron state.

Because we have the full CI solutions of the two-electron eigenstates, we can analyze the changes in electronic structure

during the relaxation by examining the CI expansion coefficients,  $(c_{n,m}^{i,+})^2$ , in eq 1. We note that once the dielectron has relaxed to its first excited state, the single two-electron product basis state that has the largest amplitude accounts for less than 50% of the total wave function, indicating that a Hartree–Fock-level (single determinant) treatment of exchange would fail to describe the excited-state dynamics of the hydrated dielectron. For comparison, the single “determinant” that dominates the ground-state singlet dielectron wave function has both electrons in their ground single-electronic states, with  $(c_{1,1}^{\text{ground},+})^2 \approx 0.77$ .<sup>19</sup>

The importance of additional configurations during the excited-state relaxation of the singlet dielectron is illustrated by the solid curve in Figure 1d, which shows the fraction of the full CI wave function in which either one or both of the electrons lie in an excited single-electron state for our representative trajectory. This “fraction excited” character, which is 23% for the equilibrium ground-state singlet dielectron,<sup>19</sup> decreases from essentially 100% immediately following excitation to between 70 and 80% once the first dielectronic excited state is occupied and reaches its quasi-equilibrium. The dashed curve shows what we call the “radical” character of the dielectron, defined as the fraction of configurations comprising the total two-electron wave function in which one electron is in the single-electron ground state and the other is in one of the single-electron excited states:  $\sum_{m=2}^N |c_{1,m}^{i,+}|^2$ . The radical character fluctuates between 50 and 70% until the dielectron reaches its quasi-equilibrated first excited state, whereupon the “radical” character rises to be almost the same as the “fraction excited” character. Finally, the dotted curve displays the “diradical” character of the excited dielectron, defined as the fraction of the total two-electron wave function comprised of configurations in which both electrons are in excited single-electron states:  $\sum_{m=2}^{N-1} \sum_{n=m}^N |c_{n,m}^{i,+}|^2$ . At equilibrium, the ground-state dielectron has  $\sim 10\%$  diradical character, as does the quasi-equilibrated first excited state, but prior to the quasi-equilibration, 15–40% of the excited state is “diradical.”

Finally, we noted in discussing Figure 3 that the charge density contours appear to suggest that the two electrons may be attempting to break apart: in other words, it appears that the dielectron might undergo photodissociation. In none of our 30 nonequilibrium trajectories, however, did we see the two electrons become separate and distinct entities (as defined by the presence of a water molecule between the two lobes and/or the exchange energy becoming zero). The separation of the two electrons requires a significant amount of solvent rearrangement, and the excited-state lifetime of the dielectron is only  $\sim 530$  fs, suggesting that the rapid nonadiabatic transition to the ground state is what prevents the dielectron from photodissociating. We tested this idea by taking the representative trajectory analyzed in Figure 1 and forcing the dielectron to stay in the first excited state for times after 500 fs (i.e., we ran adiabatic dynamics on the first excited state and did not allow nonadiabatic transitions).<sup>38</sup> After remaining on the excited state for more than 1 ps, the two lobes of the excited singlet dielectron separated, eventually reaching distances of  $\sim 8$  Å. As the interelectron separation increased, the energy difference between the ground and occupied first excited-state shrank to  $\sim 0.3$  eV, and the interelectron separation began to oscillate between between  $\sim 8$  Å and the original quasi-equilibrated excited-state separation of  $\sim 5.5$  Å; for the larger separations, the exchange energy fell to nearly zero, showing that such configurations indeed comprise separated, individual electrons. The oscillations result from a change in ordering of the two lowest-lying states as the energy

of the ground state, which occupies a single cavity, becomes greater than the energy of what had been the first excited state, which occupies two cavities. In the presence of such crossings, it makes no sense to constrain the system to a single adiabatic energy surface, so we terminated the trajectory. It is interesting to note, however, that photoexcitation is able to dissociate the dielectrons, provided they are kept in the excited state artificially. The fact that the electrons would dissociate if the transition to the ground state did not take place more quickly than the solvent can calve a second cavity has important implications for the pump–probe spectroscopy of singlet dielectrons: As we will discuss in Paper II,<sup>46</sup> the partial dissociation of the dielectron following excitation creates a distinct spectral signature that could be used to experimentally verify the existence of dielectrons, even in the presence of a large number of hydrated electrons.

**B. Relaxation Dynamics of the Photoexcited Triplet Hydrated Dielectron.** As mentioned above, our calculations of the energetics of the triplet hydrated dielectron suggest that it is not thermodynamically stable, and thus is unlikely to exist experimentally.<sup>33</sup> Nevertheless, the triplet hydrated dielectron is kinetically stable in our simulations, providing us with an opportunity to explore how changing the spin of the system affects both the nonadiabatic and solvent relaxation dynamics following excitation.

*1. Results: Full-CI Nonadiabatic Nonequilibrium Mixed Quantum/Classical Trajectories of Triplet Hydrated Dielectrons.* Figure 4a shows the dynamical history of the adiabatic eigenstates (alternating solid and dashed gray curves) and the occupied mean-field state (heavy solid curve) for a representative nonequilibrium trajectory following 4.0 eV excitation of the equilibrated triplet hydrated dielectron. In this trajectory, following promotion of the equilibrium triplet dielectron to the (resonant) ninth excited state at  $t = 0$ , strong mixing of the densely spaced excited energy levels leads to rapid nonadiabatic relaxation. Upon reaching the first excited state, the energy of the occupied state decreases rapidly, so that within a few tens of femtoseconds the ground and first excited states become nearly degenerate. This near degeneracy allows the nonadiabatic transition from the first excited state to the ground state to take place much more quickly for the triplet dielectron than for the singlet dielectron because there is no excited-state “equilibrium” gap for the triplet dielectron. For this trajectory, once the ground state is reached at  $\sim 160$  fs, the gap between the ground and first excited states opens in just a few hundred femtoseconds, so that the triplet dielectron returns to equilibrium fairly rapidly after repopulating the ground state. Figure 5a shows the energies of the occupied excited state and ground state as a function of time after excitation averaged over all 30 of the nonequilibrium trajectories.<sup>34</sup> The shift of the average excited-state energy results primarily from the rapid relaxation that follows arrival in the first excited state. Since the average excited-state lifetime is short, the levels do not reach quasi-equilibrium in the excited state as was observed for the singlet dielectron in Figure 2a.

Because the equilibrated ground state of the triplet dielectron has a peanut-shaped charge density (cf.  $t = 0$  contour plot in Figure 6, below), the radius of gyration is not a useful measure of its size and shape. Thus, we use the principal moments of inertia of the electron density to monitor the size and shape changes that take place during the relaxation of the excited triplet dielectron.<sup>19</sup> Figure 4b shows the square roots of the principal moments of inertia (solid curves) and the electron–electron separation ( $r_{12}$ , dashed curve) of the occupied state for the nonequilibrium trajectory whose adiabatic eigenstates are shown

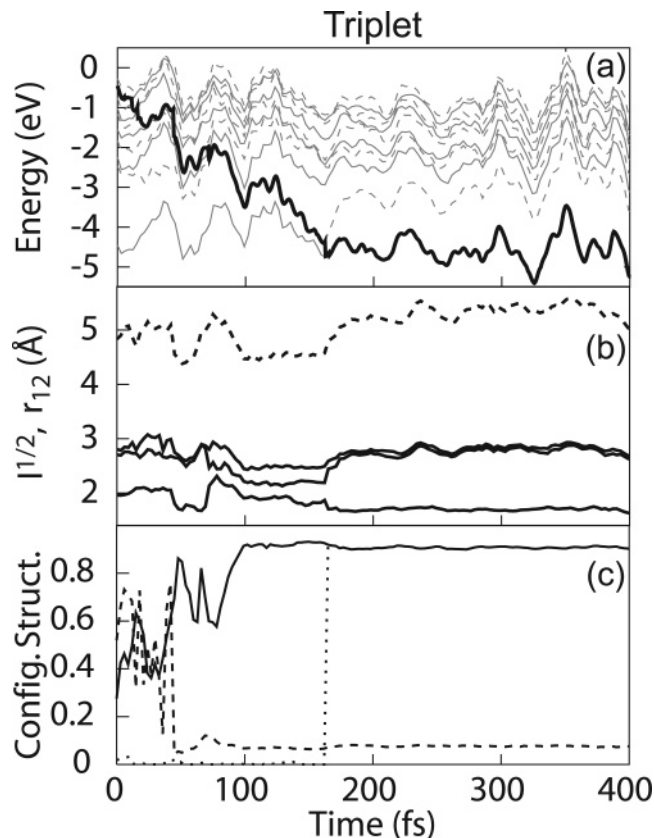


**Figure 4.** Representative dynamical history of nonadiabatic relaxation by a triplet dielectron, following resonant 4.0 eV excitation at time  $t = 0$ . Panel a: Adiabatic energy levels (alternating thin gray solid and dashed curves) and mean-field energy (thick black curve). Panel b: Geometry of the occupied-state charge density. Plotted are the interelectron separation, ( $r_{12}$ , dashed curve), and the square roots of the three moments of inertia of the charge density ( $I^{1/2}$ , solid curves), calculated as described in ref 19. Panel c: Fraction of single-determinant (solid curve), diradical (dashed curve) and  $|1,2\rangle$ - (dotted curve) character of the occupied adiabatic eigenstate.

in Figure 4a. Upon excitation, the larger moments of inertia do not change, indicating that the “length” of the excited triplet dielectron is the same as the ground state. The smallest moment of inertia increases by  $\sim 30\%$ , however, implying that the excited triplet dielectron is significantly “thicker” than the ground state. As the triplet dielectron relaxes through the higher-lying adiabatic states, the dielectron becomes longer but keeps its extra girth. After reaching the first excited state, the dielectron then shrinks in both length and average radius before returning to the ground state. The dashed curve in Figure 4b shows that for our representative trajectory, the interelectron separation does not change as dramatically as the principal moments of inertia. At the instant of excitation, the interelectron separation shrinks but then increases slightly upon solvation to end up fluctuating about the ground-state equilibrium value; thus, there is no significant change in the interelectron separation following the nonadiabatic transition to the ground state. We also found that the Coulomb and exchange energies of the triplet dielectron do not change appreciably during the nonadiabatic relaxation, which is consistent with the small change in the interelectron separation, so we do not display these energies in Figure 4.

To better visualize the geometric changes that take place during the nonequilibrium relaxation of the triplet dielectron, Figure 6 displays charge density contours of the occupied excited (yellow) and ground (red) adiabatic states at a few select times for the same trajectory studied in Figures 4a and 4b. Immediately following excitation, the narrow waist in the peanut-shaped

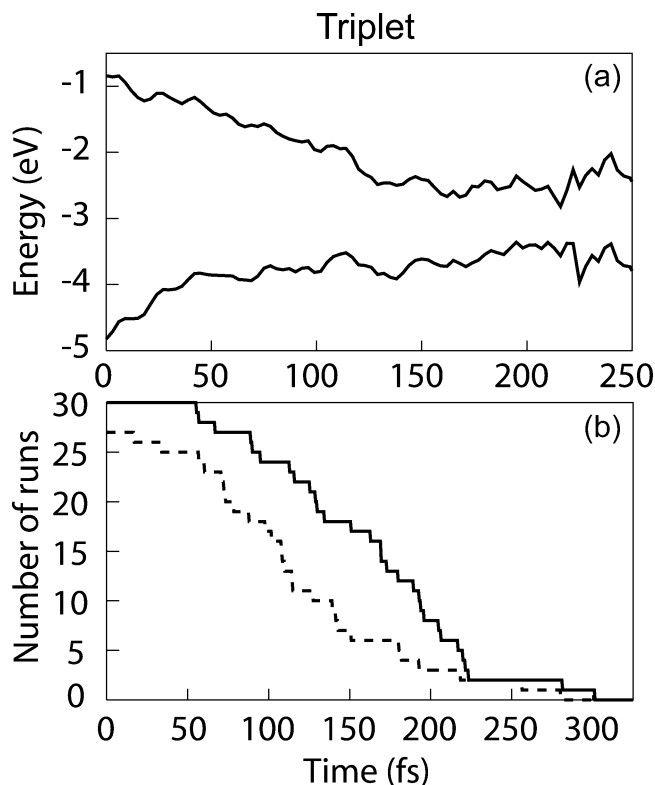


**Figure 5.** Nonequilibrium average dynamics for triplet dielectron relaxation following 4.0 eV resonant excitation at time  $t = 0$ . Panel a: Average energies of the occupied state and ground state after excitation (solid curves).<sup>34</sup> Panel b: Number of triplet-dielectron runs above the ground state (solid curve) and above the first excited state (dotted curve) as a function of time after excitation. As discussed in the text, only those 27 runs which pass through the first excited state are included in calculating the number above the first excited state.

ground state disappears; this shows that the excited-state charge density pushes out the water molecules that occupy this region in the ground state. The density contours 120 fs after excitation show that both the ground state and the occupied second excited state occupy the same cavity. By the time of the transition to the ground state at  $\sim 162$  fs, the ground and first excited states are nearly degenerate, consisting of two orthogonal but nearly identical charge distributions occupying an oblate-spheroidal cavity.

Finally, we examine the excited-state lifetimes of the 30 nonequilibrium triplet dielectron trajectories. Figure 5b shows the excited-state survival probability (solid curve) and the probability for the system to occupy an excited state higher than the first excited state (dashed curve) as a function of time after excitation. In contrast to the rapid relaxation to the first excited state followed by the slow transition to the ground state that we observed for the singlet dielectron in Figure 2c, Figure 5b reveals a relatively slow decay to the first excited state and a fast transition to the ground state for the excited triplet dielectron. The net result is that the triplet dielectron reaches the ground state much more quickly than the singlet dielectron: Table 1 shows that the average time for the triplet dielectron to reach the ground state is  $\sim 160$  fs, one third the time taken by the singlet dielectron. We found the overall rapid return to the ground state to be somewhat surprising, given that Figure 5b shows that triplet dielectrons relax to the first excited state in  $\sim 120$  fs,  $\sim 25\%$  more slowly than singlet dielectrons. Thus, the shorter overall excited-state lifetime of triplet dielectrons is due to the much smaller residency time ( $\sim 50$  fs) in the first excited state. We turn in the next subsection to question

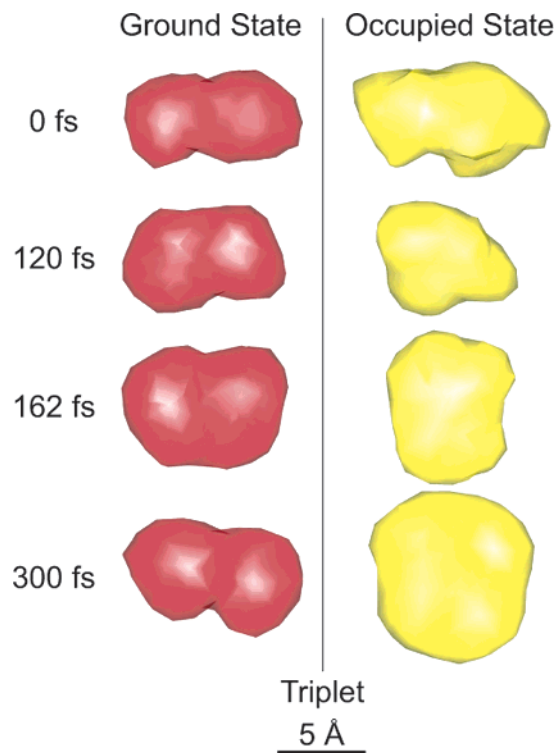


**Figure 6.** Charge density contours of the occupied and ground state for the triplet run shown in Figure 4. The ground state charge density is displayed in red and the occupied state charge density in yellow; in both cases the contours are drawn at a charge density of 10% of the maximum charge density for the state displayed. The “occupied state” contour at time  $t = 300$  fs displays the *unoccupied* first excited state, because the occupied state at this time is the ground state.

of why the relaxation dynamics of the triplet dielectron are so different from that of the singlet dielectron.

**2. Discussion: The Role of Spin in the Condensed-Phase Relaxation Dynamics of the Triplet Dielectron.** In this section, we examine in detail how the electronic structure of the excited triplet dielectron leads to very different relaxation dynamics from the singlet dielectron. Although the shape changes of the charge density following excitation are not as dramatic for the triplet dielectron as for the singlet, the excited triplet dielectron does undergo significant dynamic changes in electronic structure. The solid curve in Figure 4c displays the fraction of the occupied state wave function,  $\Psi_i$ , that can be described by a single determinant, that is, by the largest  $|c_{n,m}^{i,-}|^2$  value in the CI expansion. The triplet dielectron becomes steadily more single-determinant in character as the relaxation proceeds, rising to  $\sim 90\%$  once the first excited state is occupied. The dashed and dotted curves in Figure 4c display the dynamical changes in the fraction of diradical character ( $\sum_{n=2}^{N-1} \sum_{m=n+1}^N (c_{n,m}^{i,-})^2$ ) and the fraction of the occupied state in the lowest-possible product state ( $|c_{1,2}^{i,-}|^2$ ), respectively. As the single-determinant character increases, the diradical character of the state also increases, indicating that the occupied state wave function is increasingly composed of configurations with neither electron in the ground state. After the transition to the first excited state at 162 fs, however, the fraction of diradical character drops discontinuously to less than 10% and displays little change thereafter. This shows that the first excited state consists mainly of configurations with one electron in the single-electron ground state and the other electron in a low-lying single-electron excited state, with a small amount of diradical character mixed in by electronic correlation.

With an understanding of the changes in electronic structure in hand, we can now explain why the triplet dielectron has such different relaxation dynamics than the singlet. The fact that at the time of the transition to the ground state the charge densities of the ground and first excited states of the triplet dielectron are perpendicular (cf. Figure 6) and nearly degenerate suggests that these two states will have very similar electronic structures. We examined the 27 nonequilibrium trajectories in which the triplet dielectron spent time in the first excited state and found that in all of them the electronic structures of the ground and first excited states at the time of the transition to the ground state are described well by a sum of just two spatially antisymmetrized 2-electron product basis states,

$$\begin{aligned}\Psi_1 &\approx A|1,2\rangle_- + \sqrt{N^2 - A^2}|1,3\rangle_- \\ \Psi_2 &\approx -\sqrt{N^2 - A^2}|1,2\rangle_- + A|1,3\rangle_-\end{aligned}\quad (2)$$

where  $N^2 = 0.91 \pm 0.02$  and  $-N \leq A \leq N$ . Because the cavity containing the first excited state triplet dielectron is oblate spheroidal, the lowest single-electron eigenstates of this cavity are similar to those of the (single) hydrated electron, with an s-like ground state (|1>) and two quasi-degenerate and orthogonal p-like excited states (|2) and |3>) with another p-like state (|4>) at higher energy.<sup>20,21</sup> Since the triplet dielectron cannot have both electrons occupying the same single-electron basis states, the lowest possible two-electron product states are |1,2) and |1,3). These two lowest two-electron states are perpendicular to each other because they are composed of one-electron p-like basis states that are also perpendicular. Thus, the two states' similar electronic structure explains the near degeneracy of their energy levels, which form a doublet because the second and third single-electron states are nearly degenerate, differing by only  $\sim 0.1$  eV. Thus, it is the formation of the oblate spheroidal cavity upon reaching the first excited state that causes the strong mixing with the ground state, leading to the rapid nonadiabatic transition.<sup>39</sup> Overall, changing the spin from singlet to triplet changes the preferred two-electron configurations composing the first excited state, leading to significant spin-dependent differences in the excited-state relaxation dynamics.

We conclude this section by exploring what happens to the triplet dielectron if we prevent the transition from the first excited state to the ground state. As with the singlet dielectron, we took a single nonadiabatic trajectory and forced the triplet dielectron to evolve adiabatically after it reached the first excited state. Unlike the singlet dielectron, however, the triplet dielectron never dissociates: the oblate spheroidal cavity is stable for the first excited state. We speculate that the stability is a result of adiabatic level repulsion, because lengthening the cavity should decrease the energy of the occupied state and cause it to drop below the ground state energy. Furthermore, although moving the electrons apart would decrease the Coulomb energy, it would also simultaneously increase the (negative) exchange energy, so there is not a strong driving force for breakup of triplet dielectrons. Thus, we see that, unlike for singlet dielectrons, the electronic structure required by spin statistics leads triplet dielectrons to be stable to dissociation even when they are confined to the first excited state.

**C. The Effects of Exchange and Correlation on Solvation Dynamics and Linear Response.** The previous section makes it clear that the exchange interaction, including spin, makes the relaxation dynamics of singlet and triplet hydrated dielectrons different from each other and from that of the hydrated electron. In this section, we explore these differences in more detail,

focusing on the specific question of how exchange affects linear response. It has been well-established that linear response fails for solutes that undergo significant changes in size and shape upon excitation.<sup>36</sup> Despite the large change in size following s-like  $\rightarrow$  p-like excitation, linear response was observed to hold following excitation of the hydrated electron,<sup>21</sup> although recent calculations have cast doubt on this conclusion;<sup>40</sup> it is possible, however, that the hydrated electron may provide another example of the "hidden" breakdown of linear response.<sup>41</sup> Given that exchange causes singlet and triplet dielectrons to behave differently than hydrated electrons, how does the spin affect the apparent validity of linear response?

The solvation dynamics responsible for the nonequilibrium relaxation following the excitation of any system are measured by the Stokes shift, which is the difference between the occupied,  $E_{\text{occ}}$ , and ground state,  $E_{\text{gnd}}$ , energies,

$$\bar{U}_{\text{gap}}(t) = \bar{E}_{\text{occ}}(t) - \bar{E}_{\text{gnd}}(t) \quad (3)$$

where the overbar indicates a nonequilibrium ensemble average following the excitation at time  $t = 0$ . In the limit of linear response, the solvent motions that cause the nonequilibrium relaxation should be identical to the regression of solvent fluctuations present at equilibrium.<sup>42</sup> Thus, if linear response is valid, the normalized solvent response function,

$$S(t) = \frac{\bar{U}_{\text{gap}}(t) - \bar{U}_{\text{gap}}(\infty)}{\bar{U}_{\text{gap}}(0) - \bar{U}_{\text{gap}}(\infty)} \quad (4)$$

should be equal to the energy gap autocorrelation function,

$$C_{\text{gap}}(t) = \frac{\langle \delta E_{\text{gap}}(t) \delta E_{\text{gap}}(0) \rangle}{\langle \delta E_{\text{gap}}(0)^2 \rangle} \quad (5)$$

where  $\delta E_{\text{gap}} = U_{\text{gap}} - \langle U_{\text{gap}} \rangle$  is the equilibrium ground-to-excited-state energy gap and the angled brackets denote an equilibrium average. For hydrated dielectrons, the calculation of  $C_{\text{gap}}(t)$  raises the question of which excited state should be used to calculate the equilibrium energy gap, especially since the nonequilibrium relaxation involves transitions between several excited states on the way to the ground state.<sup>34</sup> In the strictest interpretation of linear response, the energy gap autocorrelation function should be identical for all excited states, but the electronic structure of the different dielectron excited states is distinct, so there is no guarantee that similar solvent fluctuations will modulate the different excited-state energies in exactly the same way. We can think of no convincing argument to use *any* particular state when there are such internal conversions, so in this section we will test linear response as follows. We will compare the nonequilibrium response function, eq 4, to the autocorrelation of the equilibrium ground-to-excited-state energy gap, eq 5, where we calculate the equilibrium gap by choosing both the lowest excited state and the average initially occupied excited state for the nonequilibrium trajectories. The equilibrium correlation functions are calculated using the 30-ps equilibrium trajectories described in ref 19.

Figure 7 shows both the nonequilibrium solvent response function,  $S(t)$ , (eq 4, solid curve), and the equilibrium energy gap autocorrelation functions (eq 5) for the gap to both the first excited state ( $C_2(t)$ , dashed curve) and the fifth excited state ( $C_6(t)$ , dotted curve) for the singlet dielectron.<sup>43</sup> The two equilibrium response functions are similar at short times and identical within the noise at longer times, consistent with the strictest interpretation of linear response. However, a comparison

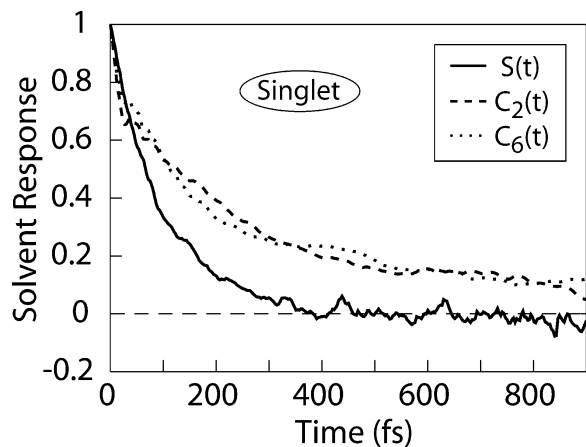


**Figure 7.** Energy gap relaxation for the singlet dielectron, showing the normalized, nonequilibrium solvent response function  $S(t)$ , eq 4 (solid curve) and the equilibrium gap autocorrelation functions, eq 5, for the ground-to-first-excited-state energy gap ( $C_2(t)$ , dashed curve) and for the ground-to-fifth-excited-state energy gap ( $C_6(t)$ , dotted curve).

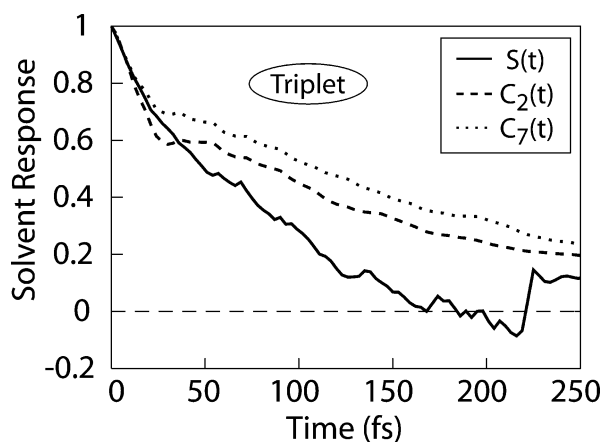


**Figure 8.** Energy gap relaxation for the triplet dielectron, showing the normalized, nonequilibrium solvent response function  $S(t)$ , eq 4 (solid curve) and the equilibrium gap autocorrelation functions, eq 5, for the ground-to-first-excited-state energy gap ( $C_2(t)$ , dashed curve) and for the ground-to-sixth-excited-state energy gap ( $C_7(t)$ , dotted curve).

of these two curves to the nonequilibrium response function shows that linear response clearly fails to describe the solvation of the excited singlet dielectron. In the nonequilibrium dynamics, the gap is narrowed by destabilization of the ground state, which requires significant translation of water molecules; Fourier transforms of  $S(t)$  and the two  $C(t)$ 's show that librations contribute significantly less to nonequilibrium than to equilibrium solvation for this system. Over the first few hundred fs, nonadiabatic transitions increase the Stokes shift and allow the nonequilibrium energy gap to close more quickly than the equilibrium energy gap decorrelates. The fact that linear response fails is perhaps not all that surprising in light of the dramatic size and shape changes the singlet dielectron undergoes upon excitation (cf. Figure 1c, above).<sup>36</sup>

A similar analysis also reveals that linear response fails to describe the solvation dynamics associated with excitation of the triplet dielectron. Figure 8 compares the normalized nonequilibrium solvent response,  $S(t)$  (eq 4, solid curve) to the equilibrium energy gap autocorrelation functions (eq 5) for both the energy gap between the ground and first excited states ( $C_2(t)$ , dashed curve) and between the ground and sixth excited states ( $C_7(t)$ , dotted curve) for the triplet dielectron.<sup>43</sup> As we saw with the singlet dielectron, the early-time nonequilibrium dynamics

of the triplet dielectron are similar to those seen at equilibrium. Once the first excited state is reached and the triplet dielectron becomes oblate spheroidal in shape, however, the nonequilibrium dynamics speed up relative to the equilibrium dynamics due to the rapid closing of the gap following the transition to the first excited state.

The results described in the previous section showed clearly that both singlet and triplet dielectrons change shape and size significantly as they relax following excitation, so that it is not surprising that their solvation dynamics do not obey linear response.<sup>36</sup> As mentioned above, what is perhaps more surprising is that the solvation dynamics of hydrated electrons has been reported to obey linear response, despite a similarly large shape change upon excitation.<sup>21</sup> The apparent applicability of linear response for the single hydrated electron cannot be ascribed to the quantum mechanical nature of the solute (since linear response fails for dielectrons), so one might suggest that the motions that drive shape changes in the nonadiabatic relaxation of hydrated electrons are the same as those that modulate the energy gaps in equilibrium. While this supposition about the motions involved in hydrated electron relaxation seems reasonable, concrete proof or disproof that this is the case would require projections of the nonequilibrium Stokes shift onto solvent motions. This can be done using a quantum mechanical generalization<sup>40</sup> of the nonequilibrium projection operator approach that was developed recently to study the breakdown of linear response in classical solvation dynamics.<sup>44</sup>

#### IV. Discussion

In summary, we have used nonadiabatic mixed quantum/classical molecular dynamics simulations to study the excited-state dynamics of hydrated dielectrons. Our computational approach allowed us to solve for the adiabatic eigenstates using full CI throughout the simulation, so we were able to monitor in unprecedented detail how solvation changed the electronic structure of this two-electron solvent-supported species. We found that photoexcitation of the singlet hydrated dielectron led to dissociation into separate single electrons if we artificially forced the dielectron to remain in its lowest electronic excited state; when we allowed for nonadiabatic relaxation, however, we found that complete dissociation never occurred because excited singlet dielectrons always make a transition to the ground state before the water can rearrange to support two independent cavities. We also found that electron correlation plays a large role in both solvation and nonadiabatic relaxation, leading to very different relaxation pathways and even different cavity shapes for singlet and triplet hydrated dielectrons. Our results for both dielectronic spin states showed that the linear response approximation failed to describe the Stokes shift dynamics for either singlet or triplet dielectrons, consistent with the significant size and shape changes after excitation.

For singlet hydrated dielectrons, we found that relaxation dynamics was faster than would be observed for the excitation of hydrated electrons with the same energy. This is because the 4.0 eV excitation of a dielectron populates an eigenstate that is bound in the same cavity as the ground state, whereas 4.0 eV excitation of the hydrated electron would lead to a continuum state. Thus, at this energy, singlet dielectron relaxation resembles relaxation by the hydrated electron after it has been excited to one of its low-lying bound excited states. Because the singlet dielectron sheds  $\sim 1$  eV of energy by nonadiabatically cascading through the excited states, its excited-state lifetime ends up being about the same as the hydrated electron's. In addition, we found that solvation dynamics

following excitation of the singlet dielectron leads to a net decrease in the electron–electron interaction energy as the electrons move apart, and that the dielectron acquires significant excited-state character as higher-lying states get called into play in order for the interelectron separation to increase.

We also found that triplet dielectrons relax to the ground state even faster than singlet dielectrons. The initial cascade through the energy levels takes longer than in the singlet case, but once the first excited state is occupied the system is nonadiabatically driven to the ground state in less than 100 fs. This rapid relaxation to the ground state is a consequence of the water being driven to form an oblate spheroidal cavity; the cavity contains two nearly-degenerate adiabatic dielectronic states (the occupied state and the ground state), so very little nonadiabatic coupling is required to induce a transition between them. Once the ground state is reached, there is no force keeping the cavity spheroidal, so the cavity rapidly expands to re-form the peanut-shaped equilibrium ground state, and in the process destroys the degeneracy. The Coulomb and exchange energies of excited triplet dielectrons do not vary much during the solvation process (most of the energy decrease resulted from changes in the cavity shape altering the single-electron energy levels), however, the electronic structure changed dramatically as the solvent relaxed. Initially, the triplet dielectron was composed of many product states, but as solvation progressed the fraction of the CI wave function that came from a single product state increased steadily. Moreover, during the relaxation, the fraction of the total wave function with either electron in the ground state decreased until the first excited state was reached, whereupon ~90% of the wave function had either  $|1,2\rangle^-$  or  $|2,3\rangle^-$  character. Shortly after reaching the ground state, the elongation of the solvent cavity returned the triplet dielectron to its usual equilibrium, with ~90% of the ground-state wave function having  $|1,2\rangle^-$  character.

We close by pointing out that the calculations we have performed for this paper demonstrate that it is possible to perform nonadiabatic excited-state molecular dynamics with full CI. This ability is noteworthy because using full CI gives access to the wave functions of both the ground and excited states, so observables such as absorption spectra may be computed directly with no approximations. In Paper II,<sup>46</sup> we take advantage of our ability to compute the ground and excited-state wave functions to compute the transient spectroscopy of photoexcited hydrated dielectrons and to predict a method for observing hydrated dielectrons using pump–probe spectroscopy. Finally, it is worth noting that the ability to do full CI calculations in solution should allow the simulation of additional processes involving electron exchange and correlation in the condensed phase that heretofore have not been accessible. In future work, we plan to perform mixed quantum/classical simulations of the dynamics of molecular photodissociation in the condensed phase from first principles, with full CI, without relying on some effective potential energy surface derived, for example, from a gas-phase electronic structure calculation.

**Acknowledgment.** This work was supported by the NSF under Grant No. CHE-0204776. R.E.L. was a California Nanosystems Institute/Hewlett-Packard Postdoctoral Fellow. B.J.S. is a Camille Dreyfus Teacher-Scholar. The charge densities shown in Figures 3 and 6 were produced using the UCSF Chimera package from the Computer Graphics Laboratory, University of California, San Francisco (supported by NIH P41 RR-01081).<sup>45</sup> We gratefully acknowledge UCLA's Academic Technology Services for the use of its Hoffman Beowulf Cluster.

## References and Notes

- (1) Classical and quantum dynamics in *Condensed Phase Simulations: Proceedings of the International School of Physics* "Computer simulation of rare events and dynamics of classical and quantum condensed-phase systems": Euroconference on technical advances in particle-based computational material sciences; Berne, B. J., Cicotti, G., Coker, D. F., Eds.; World Scientific: Singapore, 1998.
- (2) Tully, J. C. *J. Chem. Phys.* **1990**, *93*, 1061.
- (3) Hammes-Schiffer, S.; Tully, J. C. *J. Chem. Phys.* **1994**, *101*, 4657. Hammes-Schiffer, S. *J. Chem. Phys.* **1996**, *105*, 2236. Kim, S. Y.; Hammes-Schiffer, S. *J. Chem. Phys.* **2003**, *119*, 4389.
- (4) Coker, D. F.; Xiao, L. *J. Chem. Phys.* **1995**, *102*, 496. Batista, V. S.; Coker, D. F. *J. Chem. Phys.* **1996**, *105*, 4033.
- (5) Prezhdo, O. V.; Rossky, P. J. *J. Chem. Phys.* **1997**, *107*, 825.
- (6) Martnez, T. J.; Ben-Nun, M.; Levine, R. D. *J. Phys. Chem.* **1996**, *100*, 7884. Ben-Nun, M.; Martinez, T. J. *J. Chem. Phys.* **2000**, *112*, 6113.
- (7) Martens, C. C.; Fang, J.-Y. *J. Chem. Phys.* **1997**, *106*, 4918. Donoso, A.; Martens, C. C. *J. Chem. Phys.* **2000**, *112*, 3980.
- (8) Szasz, L. *Pseudopotential Theory of Atoms and Molecules*; Wiley-Interscience: New York, 1985.
- (9) Sheu, W. S.; Rossky, P. J. *J. Chem. Phys. Lett.* **1993**, *202*, 186. *J. Am. Chem. Soc.* **1993**, *115*, 7729. Sheu, W. S.; Rossky, P. J. *J. Phys. Chem.* **1996**, *100*, 1295.
- (10) Bradforth, S. E.; Jungwirth, P. *J. Phys. Chem. A* **2002**, *106*, 1286.
- (11) McQuarrie, D. A. *Quantum Chemistry*; University Science Books: Mill Valley, 1983.
- (12) Muñio, P. L.; Callis, P. R. *J. Chem. Phys.* **1994**, *100*, 4093.
- (13) Blair, J. T.; Westbrook, J. D.; Levy, R. M.; Krogh-Jespersen, K. *J. Chem. Phys. Lett.* **1989**, *154*, 531. Blair, J. T.; Krogh-Jespersen, K.; Levy, R. M. *J. Am. Chem. Soc.* **1989**, *111*, 6948.
- (14) Duncan, W. R.; Stier, W. M.; Prezhdo, O. V. *J. Am. Chem. Soc.* **2005**, *127*, 7941.
- (15) Burke, K.; Werschnik, J.; Gross, E. K. U. *J. Chem. Phys.* **2005**, *123*, 062206.
- (16) Fueki, K. *J. Chem. Phys.* **1969**, *50*, 5381.
- (17) Kaukonen, H.-P.; Barnett, R. N.; Landman, U. *J. Chem. Phys.* **1992**, *97*, 1365.
- (18) Larsen, R. E.; Schwartz, B. J. *J. Chem. Phys.* **2003**, *119*, 7672.
- (19) Larsen, R. E.; Schwartz, B. J. *J. Phys. Chem. B* **2004**, *108*, 11760.
- (20) Rossky, P. J.; Schnitker, J. *J. Phys. Chem.* **1988**, *92*, 4277.
- (21) Schwartz, B. J.; Rossky, P. J. *J. Chem. Phys.* **1994**, *101*, 6902.
- (22) Turi, L.; Borgis, D. *J. Chem. Phys.* **2002**, *117*, 6186.
- (23) Schwartz, B. J.; Rossky, P. J. *J. Phys. Chem.* **1994**, *98*, 4489, **1995**, *99*, 2953. Schwartz, B. J.; Rossky, P. J. *J. Chem. Phys.* **1994**, *101*, 6917. Schwartz, B. J.; Rossky, P. J. *Phys. Rev. Lett.* **1994**, *72*, 3282. Schwartz, B. J.; Rossky, P. J. *J. Mol. Liq.* **1995**, *65–6*, 23. Schwartz, B. J.; Bittner, E. R.; Prezhdo, O. V.; Rossky, P. J. *J. Chem. Phys.* **1996**, *104*, 5942. Wong, K. F.; Rossky, P. J. *J. Phys. Chem. A* **2001**, *105*, 2546. Wong, K. F.; Rossky, P. J. *J. Chem. Phys.* **2002**, *116*, 8418. Wong, K. F.; Rossky, P. J. **2002**, *116*, 8429.
- (24) Chandler, D.; Leung, K. *Annu. Rev. Phys. Chem.* **1994**, *45*, 557.
- (25) Neria, E.; Nitzan, A.; Barnett, R. N.; Landman, U. *Phys. Rev. Lett.* **1991**, *67*, 1011.
- (26) Allen, M. P.; Tildesley, D. J. *Computer Simulation of Liquids*; Oxford University Press: London, 1992.
- (27) Steinhauser, O. *Mol. Phys.* **1982**, *45*, 335.
- (28) We taper the electron–water interactions smoothly to zero instead of applying Ewald summation for the electron–water interaction because it is not clear how to apply Ewald summation when solving for the quantum electronic eigenstates without having to solve for the electronic eigenstates iteratively. Our neglect of the Ewald summation will lead to incorrect absolute energies (see, e.g., Peter, C.; van Gunsteren, W. F.; Hunenberger, P. H. *J. Chem. Phys.* **2003**, *119*, 12205), but we do not expect much effect on either the calculated energy gaps or dynamics. Since the two electrons share a single cavity at all times in our calculations, they should not see periodic images of each other, so we also do not need to use Ewald summation for the direct electron–electron interaction.
- (29) Toukan, K.; Rahman, A. *Phys. Rev. B* **1985**, *31*, 2643.
- (30) Webster, F.; Rossky, P. J.; Friesner, R. A. *Comput. Phys. Commun.* **1991**, *63*, 494.
- (31) We note that using 10 single-electron basis states gives energy-conserving dynamics in the ground state, but that energy conservation is significantly worse in the excited states. Using 12 basis states restores energy conservation over long times, but because most runs spend less than 1 ps in the excited state, we used only 10 states in order to speed up the calculation. Over short times (less than ~200 fs), the adiabatic dielectron states were found to have the same dynamics whether we used 10 or 12 single-electron basis states.
- (32) Equation A1 of ref 18 has a typographical error: what is written as  $\langle \Psi_j | \partial \Psi_i / \partial t \rangle$  should be written  $\langle \Psi_i | \partial \Psi_j / \partial t \rangle$ .
- (33) Larsen, R. E.; Schwartz, B. J. *J. Phys. Chem. B* **2006**, *110*, 1006.

(34) As individual trajectories reach the ground state they are removed from the ensemble, so that long-time data has much poorer statistics than short-time data.

(35) The single-exponential fits were performed using the built-in fitting routines in the Origin graphical analysis program. The average ground-state energy was fitted for times less than 900 fs to the function  $(-2.15 e^{(-t/\tau)} - 3.85)$  eV, with  $\tau = 134$  fs and  $R^2 = 0.94$ . The average occupied excited-state energy was fitted for times less than 600 fs to the function  $(0.94 e^{(-t/\tau)} - 2.92)$  eV, with  $\tau = 50$  fs and  $R^2 = 0.66$ . The normalized energy difference between the ground and occupied states was fitted for times less than 900 fs to the function  $e^{(-t/\tau)}$  with  $\tau = 100$  fs and  $R^2 = 0.996$ .

(36) Aherne, D.; Tran, V.; Schwartz, B. J. *J. Phys. Chem. B* **2000**, *104*, 5382.

(37) We define the exchange energy as in ref 18, such that a two-electron wave function with both electrons in the same state splits the total electron-electron interaction into half Coulomb and half exchange energy. This definition means that when the two separated single electron cavities have precisely degenerate energies, the Coulomb energy drops by a factor of 2 and the exchange energy increases by the amount of the decrease; the total interaction is continuous.

(38) To conserve energy over several picoseconds with the singlet dielectron fixed to be in the first excited state, we found it necessary to use

12 single-electron states in the CI calculation and to update the important states every 2 ps instead of every 3 ps: see Note 31.

(39) A similar configuration of perpendicular charge densities and a rapid transition to the ground state was also seen in ref 18 when the triplet dielectron was excited directly to its first excited state.

(40) Bedard-Hearn, M. J.; Larsen, R. E.; Schwartz, B. J., in preparation.

(41) Bedard-Hearn, M. J.; Larsen, R. E.; Schwartz, B. J. *J. Phys. Chem. A* **2003**, *107*, 4773.

(42) Chandler, D. *Introduction to Modern Statistical Mechanics*; Oxford University Press: New York, 1987.

(43) The averaging in Figures 7 and 8 is performed using only those trajectories that are still in an excited state at each time, cf. Figures 2c and 5b.

(44) Bedard-Hearn, M. J.; Larsen, R. E.; Schwartz, B. J. *J. Phys. Chem. B* **2003**, *107*, 14464.

(45) Huang, C. C.; Couch, G. S.; Pettersen, E. F.; Ferrin, T. E. *Pacific Symposium on Biocomputing* **1996**, *1*, 724. The Chimera code is freely available on the worldwide web at <http://www.cgl.ucsf.edu/chimera>.

(46) Larsen, R. E.; Schwartz, B. J. *J. Phys. Chem. B* **2006**, *110*, 9692.